Identification of Xin-repeat proteins as novel ligands of the SH3 domains of nebulin and nebulette and analysis of their interaction during myofibril formation and remodeling

Stefan Eulitz[a], Florian Sauer[b,*], Marie-Cecile Pelissier[b], Prisca Boisguerin[c,†], Sibylle Molt[a], Julia Schuld[a], Zacharias Orfanos[a], Rudolf A. Kley[d], Rudolf Volkmer[c], Matthias Wilmanns[b], Gregor Kirfel[a], Peter F. M. van der Ven[a], and Dieter O. Fürst[a]

[a]Institute for Cell Biology, University of Bonn, D-53121 Bonn, Germany; [b]European Molecular Biology Laboratory-Hamburg/Deutsches Elektronen-Synchrotron, D-22603 Hamburg, Germany; [c]Department of Medicinal Immunology, Charité-University Medicine Berlin, D-13353 Berlin, Germany; [d]Department of Neurology, Neuromuscular Center Ruhrgebiet, University Hospital Bergmannsheil, Ruhr-University Bochum, D-44789 Bochum, Germany

ABSTRACT The Xin actin-binding repeat–containing proteins Xin and XIRP2 are exclusively expressed in striated muscle cells, where they are believed to play an important role in development. In adult muscle, both proteins are concentrated at attachment sites of myofibrils to the membrane. In contrast, during development they are localized to immature myofibrils together with their binding partner, filamin C, indicating an involvement of both proteins in myofibril assembly. We identify the SH3 domains of nebulin and nebulette as novel ligands of proline-rich regions of Xin and XIRP2. Precise binding motifs are mapped and shown to bind both SH3 domains with micromolar affinity. Cocrystallization of the nebulette SH3 domain with the interacting XIRP2 peptide PPPTLPKPKLPKH reveals selective interactions that conform to class II SH3 domain–binding peptides. Bimolecular fluorescence complementation experiments in cultured muscle cells indicate a temporally restricted interaction of Xin-repeat proteins with nebulin/nebulette during early stages of myofibril development that is lost upon further maturation. In mature myofibrils, this interaction is limited to longitudinally oriented structures associated with myofibril development and remodeling. These data provide new insights into the role of Xin actin-binding repeat–containing proteins (together with their interaction partners) in myofibril assembly and after muscle damage.

INTRODUCTION

The formation of the highly ordered contractile apparatus of cross-striated muscle is a paradigm for macromolecular assembly and results in an almost crystalline arrangement of its components. This stepwise process begins with the assembly of precursor structures, premyofibrils, which subsequently progressively mature via nascent myofibrils into functional myofibrils (Rhee et al., 1994; Sanger et al., 2002, 2010). The initially formed muscle-specific, protein-containing structures mainly contain proteins that are known to be prominent components of the sarcomeric Z-disc, such as α-actinin 2, filamin C, and myopodin (van der Ven et al., 2006; Linnemann et al., 2010; Sanger et al., 2010). Because they resemble dense bodies, they are called Z-bodies. Actin filaments, associated with troponin and tropomyosin, are connected in these Z-bodies and interdigitate with

nonmuscle myosin II filaments. Incorporation of essential myofibril-lar proteins like titin or nebulin and replacement of nonmuscle myosin II by muscle myosin II isoforms are subsequent steps of myofibril maturation. The lateral alignment and fusion of Z-bodies creates early Z-bands, which represent the initial characteristic signs of formation of the highly regular sarcomere array (Sanger et al., 2010).

One of the earliest striated muscle proteins expressed during muscle development is Xin, which is revealed already in muscle precursor cells very early during embryonic development (Wang et al., 1999; Gustafson-Wagner et al., 2007; Otten et al., 2010) and in activated satellite cells (Hawke et al., 2007). It belongs to the Xin actin-binding repeat–containing protein (XIRP) family, comprising striated muscle-specific multiadapter proteins. In mammals these proteins are encoded by two genes (XIRP1, XIRP2), giving rise to the proteins Xin and XIRP2, respectively. Whereas intraexonic splicing generates three human Xin variants (van der Ven et al., 2006), only one isoform has been described for human XIRP2 (Huang et al., 2006; McCalmon et al., 2010; Wang et al., 2010), although also for this gene several database entries indicate the expression of several distinct isoforms as a result of alternative splicing. The largest Xin isoform (XinA) and XIRP2 share a similar domain organization, starting with an amino-terminal, proline-rich region that binds EVH1 domains (van der Ven et al., 2006) and a varying number of Xin repeats, followed by clusters of proline-rich motifs containing several putative SH3 domain–binding portions (Wang et al., 1999, 2010; Pacholsky et al., 2004; van der Ven et al., 2006). Whereas the Xin repeats define a novel F-actin–binding motif (Pacholsky et al., 2004), the function of most of the proline-rich clusters is unknown.

Nebulin is almost exclusively expressed in skeletal muscle, and for a long time it was considered to serve as a ruler determining thin filament length (Labeit et al., 1991; McElhinny et al., 2005; Witt et al., 2006). Recent results challenge that view, however, and instead point to a function as a stabilizer of thin filaments (Castillo et al., 2009; Pappas et al., 2010, 2011). In cardiac muscle, the related protein nebulette is predominantly expressed. In comparison to nebulin, nebulette is much smaller in size, but both proteins exhibit a highly similar domain organization, with an acidic region at the amino terminus that is followed by nebulin-like repeats. The difference in protein length is mainly explained by the absence of nebulin superrepeats in nebulette (Pappas et al., 2011). At their carboxy terminus both nebulin and nebulette contain an SH3 domain, which is connected to the repeats by a serine-rich linker sequence (Labeit and Kolmerer, 1995; Moncman and Wang, 1999; Panaviene and Moncman, 2007). The SH3 domains of both proteins are inserted into the Z-disc and are proposed to interact with myopalladin, α-actinin, and titin, although direct proof is missing (Nave et al., 1990; Moncman and Wang, 1999; Politou et al., 2002; Ma and Wang, 2002; Ma et al., 2006). The amino terminus of nebulin extends to close to the pointed end of thin filaments, where it interacts with tropomodulin (McElhinny et al., 2001). Although nebulin transcripts were also detected in cardiac muscle, the expression of the protein seems to be greatly reduced, and its distribution in cardiac muscle cells is unknown (Kazmierski et al., 2003; Joo et al., 2004). In contrast, nebulette, which was presented as a candidate gene for dilated cardiomyopathy (Purevjav et al., 2010), is exclusively expressed in cardiac muscle. The function of nebulette in the heart is unclear. The protein is associated with early premyofibrillar structures in the developing chicken heart, indicating a role during early stages of myofibrillogenesis (Esham et al., 2007). On expression of nebulette fragments in cultured cardiomyocytes, nebulette and its binding partner tropomyosin are removed from the myofibrils,

resulting in an impairment of beating (Moncman and Wang, 2002). A splice variant of nebulette (LASP-2, also called LIM-nebulette) was described as a novel actin-organizing protein of the Z-disc (Li et al., 2004; Zieseniss et al., 2008). This protein contains the serine-rich linker and the SH3 domain of nebulette linked to a LIM domain and might be involved in assembly and stabilization of the Z-disc. The SH3 domains of nebulin and nebulette are highly homologous and share at least α-actinin as an overlapping binding partner. Furthermore, the nebulette SH3 domain also targets to the myofibrillar Z-disc, underlining their similarity (Moncman and Wang, 1999).

Here we present Xin and XIRP2 as novel ligands of the SH3 domains of nebulin and nebulette. Specific proline-rich regions are identified as binding sites in both proteins, and the consensus sequence for the binding motif is found to be PPXXXPKP, which conforms to class II peptides. The molecular mechanism of binding is confirmed by a high-resolution structure of the nebulette SH3 domain with the identified XIRP2 peptide motif. The colocalization of Xin and XIRP2 with nebulin and nebulette in differentiating striated muscle cells and in areas of myofibrillar remodeling in adult muscle fibers indicate that these protein interactions are important for processes during which myofibrils are built or rebuilt.

RESULTS

Xin-repeat proteins are novel ligands of nebulin and nebulette SH3 domains

To identify interaction partners of the proline-rich regions 3 and 4 in human Xin, we screened a skeletal muscle cDNA library in a yeast two-hybrid assay using a Xin fragment encompassing amino acids 1120–1416 of XinA (Xin PR3+4) as bait (Figure 1A). Fourteen of 27 sequenced double-positive clones encoded portions of the carboxy terminus of nebulin. The smallest clone contained only part of the serine-rich linker sequence and the SH3 domain, suggesting an interaction of the proline-rich motifs of Xin with the SH3 domain of nebulin (Figure 1B). Because the bait contained two proline-rich clusters, one located in a region specific for XinA (PR3) and the second in the amino terminus of XinC (PR4), we performed additional yeast two-hybrid experiments using XinB and XinC as baits. Whereas XinB did not bind, XinC interacted with nebulin, which mapped the binding motif to the amino terminus of XinC (Figure 2). Thus both XinA and XinC harbor the interaction site to nebulin. Of note, none of the other preys encoded a protein with an SH3 domain.

Owing to the highly similar domain layout with Xin, we also tested a XIRP2 fragment encompassing amino acids 2045–2226 (isoform 4, Accession Number NP_001186073), containing five proline-rich clusters situated carboxy terminal of the repeats (XIRP2 PR2-6). Indeed, this fragment also bound nebulin in a yeast two-hybrid assay, thus identifying specific isoforms of both members of the human XIRP family as novel ligands of nebulin (Figure 2).

The high proline content of the binding regions in Xin and XIRP2 suggested a proline-based interaction with the SH3 domain of nebulin that is highly homologous to the SH3 domain of the related protein nebulette. Therefore we investigated whether Xin and XIRP2 also bind nebulette. Yeast two-hybrid assays demonstrated that a nebulette fragment containing its serine-rich linker sequence and the SH3 domain (NET SH3+L) was also capable of binding both XIRPs (Figure 2).

Biochemical confirmation of the interaction of Xin-repeat proteins with nebulin and nebulette

The highly insoluble nature of nebulin precluded verification by co-precipitation from muscle tissue of the foregoing findings. To substantiate the results obtained by yeast two-hybrid assays, we instead
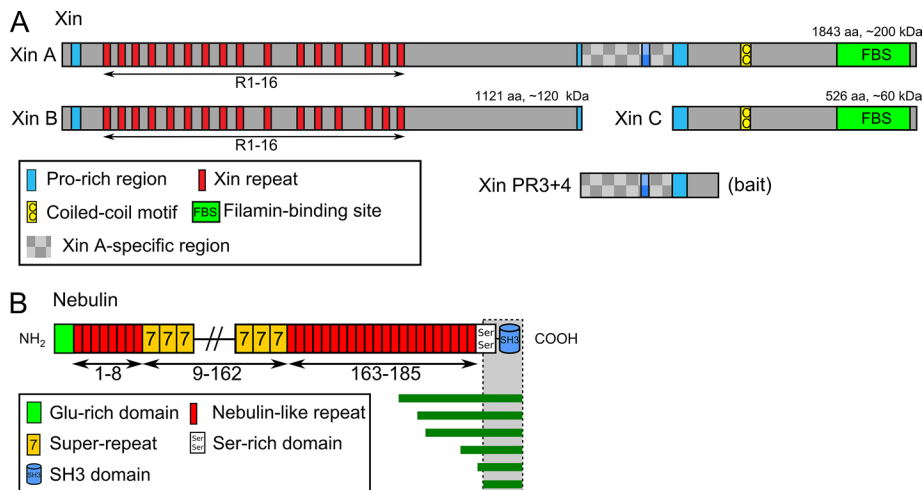
FIGURE 1: Schematic representation of domain structures of Xin isoforms and nebulin. (A) Molecular layout of the three known Xin variants and the bait construct used for the yeast two-hybrid screen (Xin PR3+4). (B) Domain organization of nebulin, together with some prey constructs (dark green bars) from the yeast two-hybrid screen. The smallest interacting construct comprises the SH3 domain and is part of the serine-rich linker. Domains are explained in the appendant boxes.

performed coimmunoprecipitation of defined protein fragments expressed in bacteria. Portions of nebulin and nebulette were expressed as amino-terminally T7-tagged proteins, and the Xin and XIRP2 fragments contained either an EEF or a c-myc tag. The purified nebulin and nebulette fragments were incubated with a single Xin or XIRP2 fragment and subsequently immunoprecipitated with an antibody directed against the T7 tag. Complex formation was analyzed using the EEF tag or the c-myc-tag antibody. These assays demonstrated that all Xin and XIRP2 fragments that bound nebulin and nebulette in yeast two-hybrid assays, for example, XinC (not shown), Xin PR4 (Figure 3, A and C), and XIRP2 PR2-6 (Figure 3, B and D), also coprecipitated with the SH3 domain–containing fragments of nebulin and nebulette.

Xin and XIRP2 interact with the SH3 domain of nebulette via conserved peptide motifs

To map the peptide motifs in Xin and XIRP2 responsible for binding to the SH3 domain of nebulette, we performed a peptide scan of the fragments Xin PR3+4 and XIRP2 PR2-6. The nebulette SH3 domain fused to glutathione S-transferase (GST) was used to overlay the immobilized peptides. Overlays using GST alone were performed as

controls for unspecific binding of the GST tag. An interaction was indicated by a signal obtained with a GST antibody. This assay identified specific proline-rich sequences in Xin (PR4; SHPPQRLPKPLP) and XIRP2 (PR6; GVLPPPTLPKPK) as SH3 domain–binding peptides (Figure 4, A and B). The specificity of the interaction with the Xin peptide SHP-PQRLPKP is highlighted by the observation that the neighboring related sequence KK-KPQLPPKP did not interact.

Of interest, both peptides do not represent a perfect match to the "classic" consensus motif of class II SH3 ligands. In Xin, the peptide lacks a PXXP sequence, and in XIRP2, the positively charged amino acids are not separated from the PXXP motif by an additional residue. To identify precisely which residues are crucial for SH3 binding, we mutated each residue to any other amino acid and used the resulting spot matrix in overlay assays. This delineated two or three essential prolines and one lysine residue in the Xin peptide motif PXXXPKP and in XIRP2 motif PXXXPKX as the sequence interacting with the SH3 domain (Figure 4, A and B). In contrast to two amino acids enframed by prolines in the "classic" PXXP SH3-binding consensus motif, in this case two essential prolines are separated by three amino acids, and the important positively charged lysine is directly enframed by prolines. Thus, in spite of the difference in the spacing of prolines, both peptide motifs suggested a binding mode similar to a typical class II ligand, which becomes more apparent in case of the Xin peptide motif.

Structure of the nebulette SH3–XIRP2 PR6 complex

To investigate the molecular details of binding, we solved the crystal structure of the nebulette SH3 domain in the presence of a synthetic 13-mer peptide (PPPTLPKPKLPKH), which contains the nebulin/nebulette binding site of XIRP2, at 1.2-Å resolution (Figure 5). The final electron density allowed the modeling of 56 of 64 residues of the SH3 domain and 11 residues of the XIRP2 peptide (residues 2245–2255). The side chains of the Lys-2253 and Leu-2254 could not be modeled because of insufficient electron density. Owing to the high resolution of the experimental data obtained, six residues of the XIRP2 peptide could be modeled with two alternate conformations. Diffraction data and refinement statistics are given in Table 1.

The structure confirms our prediction that XIRP2 acts as a class II ligand to the nebulette SH3 domain. In the structure, XIRP2 adopts a right-handed polyproline helix conformation and covers a surface of ~450 Å^2 on the nebulette SH3 domain. Lys-2251 of the XIRP2 peptide forms specific interactions with two negatively charged residues (Asp-971, Glu-972) from the RT loop that has two additional negatively charged residues preceding those involved in XIRP2 binding (Asp-969, Glu-970). Such negatively charged residue cluster in an SH3 domain RT loop is unusual and explains why the nebulette SH3 domain is capable of binding the XIRP2 peptide motif that has a lysine directly following the second invariant proline as opposed to

FIGURE 2: Summary of yeast two-hybrid analysis of interaction with Xin-repeat proteins. Combinations of baits and preys examined in yeast two-hybrid assays and the experimental results (+, –, interaction and no interaction, respectively). Note that proline-rich regions of both Xin and XIRP2 bind to the carboxy terminus of nebulin and nebulette.
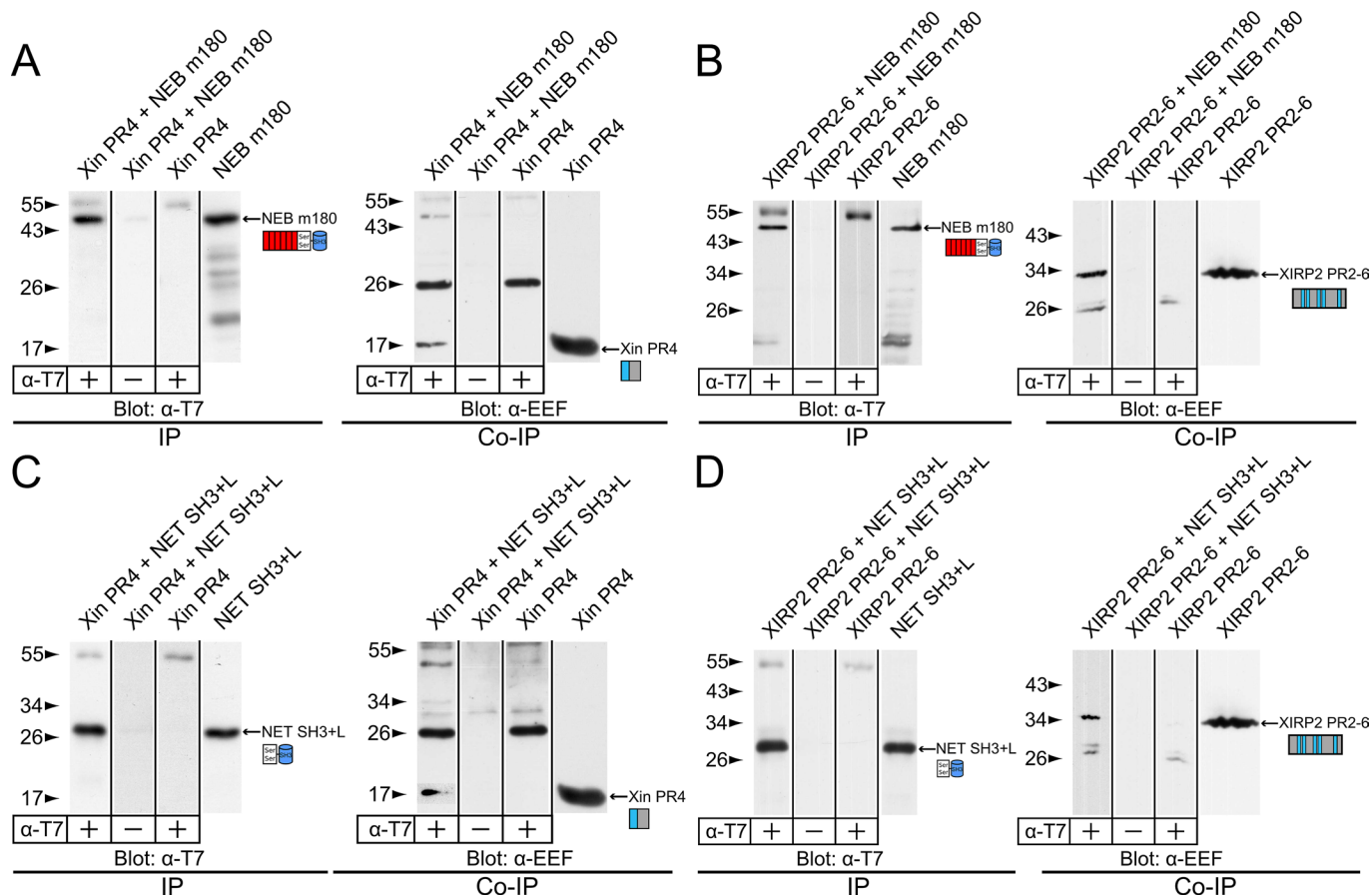
FIGURE 3: Biochemical verification of the interaction of Xin-repeat proteins with nebulin and nebulette in coimmunoprecipitation (coIP) assays. Recombinant fragments of nebulin (NEB m180) and nebulette (NET SH3+L) were mixed with fragments of Xin (PR4) or XIRP2 (PR2-6) as indicated at the top of each lane and precipitated with (+) or without (–) the T7 mAb (blot: IP). Binding of Xin (A, C) or XIRP2 (B, D) fragments was demonstrated by staining duplicate blots with an antibody against their respective tags (myc tag or EEF tag) marked with coIP. All fragments of Xin and XIRP2 were coprecipitated both with nebulin and nebulette fragments. Controls without antibody and/or interaction partner confirmed specific binding. Numbers at the left indicate positions of molecular mass markers in kilodaltons, and arrows show the positions of the individual constructs.

the classic PXXPX(K/R) class II binding motif, in which the two residues are inserted by an additional variable amino acid. Crystallographic data have been submitted to the Protein Data Bank (www.rcsb.org/pdb/explore/explore.do?structureId=4F14).

Quantitative evaluation of the interaction of XIRP2 with nebulin/nebulette SH3 domains

To further characterize the interaction of the nebulin and nebulette SH3 domains with the binding peptide of XIRP2, we investigated their specific binding parameters using isothermal microcalorimetry (ITC). Our measurements revealed 1:1 stoichiometry and a dissociation constant of 9.3 and 12.9 μM for nebulin and nebulette, respectively (Table 2 and Supplemental Figure S1), implying no significant differences between nebulin and nebulette with respect to their binding mode to XIRP2.

Immunolocalization of Xin and nebulin in differentiating skeletal muscle cells

To gain insight into the biological function of the Xin–nebulin interaction, we double stained differentiating mouse myocytes fixed at different developmental stages for both proteins with antibodies recognizing the nebulin modules M176–M181 located in the Z-disc

region and the repeat region of Xin, respectively. All cells were analyzed by confocal or spinning disc microscopy.

At early developmental stages Xin was associated with actin filaments in a continuous manner and in part colocalized with nebulin (Figure 6, A–C, inset, arrowheads). In contrast, many structures in the periphery of the cells (either adhesion plaques or nonstriated premyofibrils) were decorated by Xin but not nebulin antibodies, indicating that Xin is associated with these structures in advance of nebulin (Figure 6, A–C, arrows). Of note, all structures containing Xin and/or nebulin were also stained with RaA653, which detects sarcomeric α-actinin, identifying these structures as (pre)myofibrils (data not shown). On progression of myogenic differentiation, nebulin expression levels increased, and the protein was mainly found associated with still nonstriated nascent myofibrils spanning the entire cell, where it extensively colocalized with Xin (Figure 6, D and H–J, arrowheads). In contrast, nascent myofibrils displaying a high level of nebulin expression in a rudimentary punctate pattern exhibited only minor Xin association. At these sites, Xin was no longer continuously decorating actin filaments and instead revealed a dot-like arrangement (Figure 6, D–G, arrows). Colocalization with a Z-disc epitope of nebulin indicates that these structures presumably represent Z-bodies. In highly differentiated, contracting myotubes,
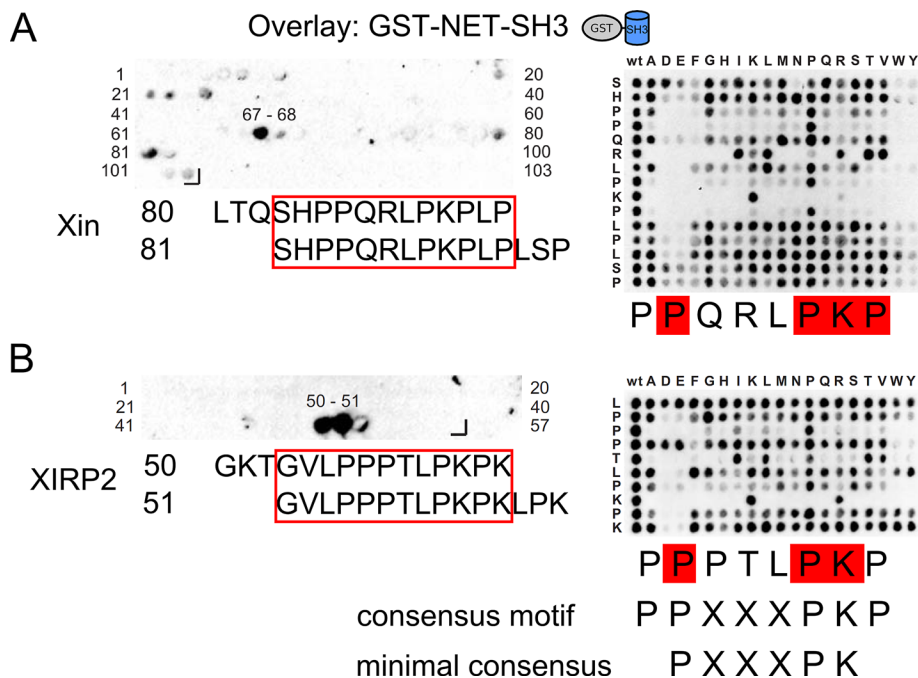
FIGURE 4: Peptide array analysis to identify the peptide motifs in Xin and XIRP2 mediating binding to the SH3 domain of nebulette. Arrays of overlapping peptides representing binding regions of Xin (A) and XIRP2 (B) were synthesized on a modified cellulose membrane and overlaid with a GST-tagged SH3 domain of nebulette. Peptides 80 and 81 of Xin and 50 and 51 of XIRP2 showed the strongest specific binding to the SH3 domain. Additional signals were observed with only GST or only secondary antibody and therefore are unspecific. Respective peptide sequences are aligned and the overlapping amino acids boxed. Right, the complete substitutional analysis, in which each amino acid of the interacting peptide (wt; *y*-axis) was exchanged for any other amino acid (spotted along the *x*-axis). Both nebulette SH3 domain–binding peptides in Xin and XIRP2 contain a proline-rich motif and a positively charged lysine residue flanking this sequence C-terminally. The established overall consensus motif therefore is PPXXXPKP, with as minimal consensus PXXXPK.

carboxy terminus of nebulette disrupted proper functioning of its SH3-domain (unpublished results), all tags were attached to its amino terminus. Complex formation was observed only upon cotransfection of Venus1-nebulette and Venus2-XinC or XinB+PR4-Venus2. No fluorescent signals were observed in combination with vectors without insert (data not shown), demonstrating the specificity of signals.

The localization of the resulting BiFC fluorescence signal was compared with the localization of the single transfections of all proteins fused to the complete Venus protein (Figure 7). On transfection into embryonic mouse cardiomyocytes, nebulette exhibited continuous decoration of nascent myofibrils, whereas in more mature myofibrils the fusion protein was targeted to Z-bodies (immature Z-discs) and Z-discs (Figure 7, A–C). In accordance with the earlier immunolocalization studies, XinC also localized mainly to nascent myofibrils. In addition, aggregates were formed, and at these sites nascent myofibrils were reduced, indicating a dominant-negative effect upon its overexpression (Figure 7, D–F). At later stages when Z-disc formation was visible, XinC specifically localized at individual longitudinal strands between adjacent Z-discs, whereas no Z-disc targeting was observed (Figure 7, G–I).

Cotransfection of Venus1-nebulette and Venus2-XinC constructs in cardiomyocytes

nebulin was localized in a highly ordered cross-striated pattern (Figure 6, K and P), whereas a prominent Xin signal was observed only as longitudinally oriented structures associated with immature Z-discs or Z-discs that were not properly aligned (Figure 6, K–Q, arrowheads). Small amounts of nebulin were also detected in these areas (Figure 6, M and P). As the maturation of the myofibrils proceeded, Xin expression dramatically decreased (Figure 6, O–Q), and the protein could hardly be detected in the contractile apparatus and became restricted to substrate attachment regions.

Subcellular localization of the Xin–nebulette interaction in embryonic mouse cardiomyocytes and C2C12 skeletal myoblasts by bimolecular fluorescence complementation

Subsequently we analyzed the expression of the interaction partners Xin and nebulette in cultured muscle cells and pinpointed their sites of interaction directly by bimolecular fluorescence complementation (BiFC; Hu *et al.*, 2002). The molecular sizes of both nebulin and XIRP2 precluded the use of full-length cDNAs, and we thus focused on the interactions between nebulette with XinB+PR4, a C-terminally extended version of XinB containing the nebulin/nebulette SH3 interaction site, and XinC, the smallest Xin isoform harboring the SH3 interaction motif. Both Xin constructs and nebulette were fused to fragments of the yellow fluorescent protein Venus (Nagai *et al.*, 2002), comprising either the amino-terminal 154 amino acids (Venus1) or residues 155–238 (Venus2), which only together form a functional fluorescent complex. Because the addition of tags to the
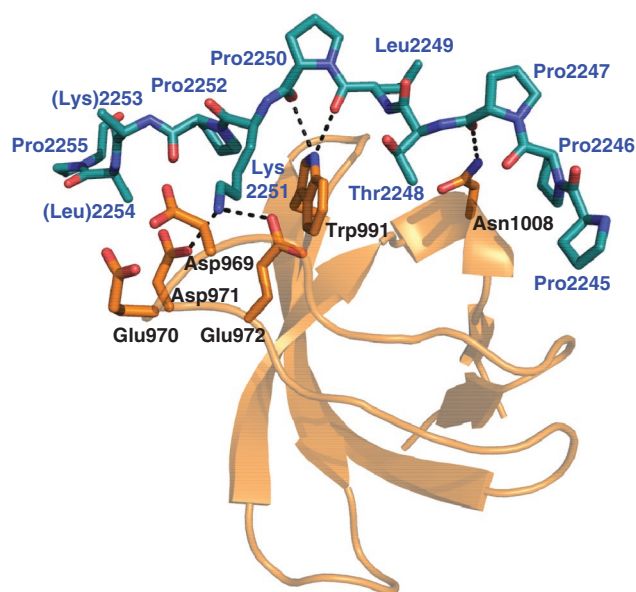

FIGURE 5: Ribbon/stick presentation of the nebulin SH3–XIRP2 peptide complex. The nebulin SH3 domain is in orange, and the XIRP2 peptide is in cyan. All visible XIRP2 residues and those nebulin SH3 domain residues that are involved in specific interactions with XIRP2 are labeled. Intermolecular hydrogen bonds are shown by dashed lines.

Characteristic	Data
Space group	$P2_12_12_1$
Cell dimensions a, b, c (Å)	35.6, 38.4, 43.3
Wavelength (Å)	0.8123
Resolution (Å)	18.5–1.2 (1.23–1.20)
Number of measured reflections	64,120 (4062)
Number of unique reflections	18,936 (1391)
Completeness (%)	98.7 (98.0)
Multiplicity	3.4 (2.9)
Mean $I/\sigma(I)$	19.2 (4.9)
R_{merge} (%)[a]	4.4 (21.4)
Refinement	
Reflections work/test set	17,984/952
R_{cryst}/R_{free} (%)[b]	14.5/17.1
Number of protein/ion/solvent atoms	571/1/104
Root-mean-square deviation bond lengths (Å)	0.011
Root-mean-square deviation angles (deg)	1. 471
Mean B-factor protein/ions/solvent (Å^2)	16.6/15.5/35.1
Ramachandran statistics	
Most /additionally favored (%)	97.1 / 2.9

Values in parentheses correspond to those from the highest-resolution shell.
[a]$R_{merge} = \sum_{hkl} \sum_i |I_i(hkl) - <I(hkl)>|/\sum_{hkl} \sum_i I_i(hkl)$, where the sum over hkl is the sum over all reflections, and the sum over i is the sum over all equivalent and symmetry-related reflections.
[b]$R_{cryst} = \sum_{hkl} \|F_{obs}\| - k|F_{calc}\| / \sum |F_{obs}|$, where F_{obs} and F_{calc} are, respectively, the observed and calculated structure factor amplitudes scaled by a scale factor k.

TABLE 1: X-ray and refinement statistics.

resulted in fluorescent complex formation at nascent myofibrils (Figure 7, J–L). There, both proteins colocalized with endogenous Xin, demonstrating an interaction at early stages of myofibril formation. On progression of myofibril development, the nebulette–XinC complex became highly restricted and was only revealed in single longitudinal strands connecting adjacent Z-discs, indicating that nebulette and Xin do not interact in mature Z-discs (Figure 7, M–O).

Highly similar results were obtained upon cotransfection of Venus1-nebulette and XinB+PR4-Venus2 in C2C12 mouse myoblasts (Figure 8). A continuous BiFC signal was mainly observed associated with nascent myofibrils that were often localized close to the sarcolemma (Figure 8, A–C). On further differentiation, the

	XIRP2–nebulin	XIRP2–nebulette
K_d (µM)	9.61 ± 0.63	12.93 ± 0.84
n	1.02 ± 0.04	1.12 ± 0.07
ΔH (kcal/mol)	–9.43 ± 0.29	–8.46 ± 0.48
$-T\Delta S$ (kcal/mol)	2.59 ± 0.27	1.79 ± 0.45
ΔG (kcal/mol)	–6.85 ± 0.04	–6.67 ± 0.04

Data are represented as the mean of three measurements ± SD.

TABLE 2: Binding parameters determined by ITC.

complex was still found at these structures (Figure 8, D–I, arrows) even after formation of Z-bodies (Figure 8, G–I, open arrows). At the same time only a weak signal was found associated with still immature, fuzzy Z-discs (Figure 8, G–I, closed arrows). In contrast, fully established Z-discs showing a bright and compact staining for a Z-disc epitope of titin were no longer decorated by a BiFC-signal (data not shown).

Xin and nebulin in remodeling skeletal muscle
The BiFC results indicate a spatiotemporally regulated and transient interaction of Xin and nebulette. In cardiomyocytes of a late developmental stage the BiFC complex was only revealed at longitudinal strands between adjacent Z-discs that are highly reminiscent of the F-actin– and desmin–containing structures detected in areas of remodeling in skeletal muscle after eccentric exercise (Yu et al., 2003, 2004). To investigate whether XIRPs are involved in remodeling of the myofibrillar apparatus, we labeled mouse and human skeletal muscle sections with antibodies against Xin and XIRP2, as well as with nebulin, filamin C, and α-actinin as Z-disc markers. Staining for Xin and XIRP2 revealed a strikingly specific decoration of longitudinal strands spanning one or more successive sarcomeres in areas where the normal Z-disc array was disrupted (Figure 9 and Supplemental Figure S2). In these areas, both nebulin and α-actinin were often not properly localized at the Z-disc and exhibited a rather diffuse distribution. A further indication for muscle remodeling at these sites were delta-shaped areas revealing supernumerary sarcomeres and misaligned myofibrils due to the addition of one or more supernumerous sarcomeres, as described in delayed-onset muscular soreness after eccentric exercise (Yu et al., 2003, 2004). Whereas Xin expression was highly restricted to these areas, minor quantities of XIRP2 also localized to mature myofibrils. Although Xin and XIRP2 are components of different structures in normal adult skeletal muscle fibers, both proteins are conspicuously enriched in remodeling areas together with their binding partner filamin C and at least partially also nebulin.

DISCUSSION
The sarcomeric Z-disc is a dense protein network that links thin myofilaments from adjacent sarcomeres into I-Z-I complexes. In addition to this structural role, the Z-disc serves as a nodal point integrating several signaling pathways (Luther, 2009; Frank and Frey, 2011). Strategies to explore signaling events at the molecular level include the search for protein–protein interactions of domains that evidently are involved in controlling signaling cascades, like the SH3 domains of Z-disc– and thin filament–associated proteins nebulin and nebulette. These proteins share a similar domain layout, and their carboxy-terminal SH3 domains are positioned at the Z-disc (Wright et al., 1993; Millevoi et al., 1998). Surprisingly few studies have addressed this interesting regulatory domain. Predictions based on the three-dimensional structure of the nebulin SH3 domain suggested peptide sequences in the Z-repeats and PEVK region of titin as potential ligands, and affinity measurements revealed reasonably high binding strengths between 0.7 and 77 µM (Politou et al., 1998, 2002; Ma and Wang, 2002; Ma et al., 2006). These were, however, in vitro studies, and evidence for an interaction in vivo is lacking.

Myopalladin was also described as a ligand of the nebulin SH3 domain, suggesting a role as part of an intra–Z-disc meshwork that connects α-actinin and titin at the periphery with the desmin intermediate filament system (Bang et al., 2001; Ma and Wang, 2002; Ma et al., 2006). The exact binding motif was predicted on the assumption of a polyproline-mediated SH3 domain interaction, and the selected peptide conforms to neither classic type I nor type II
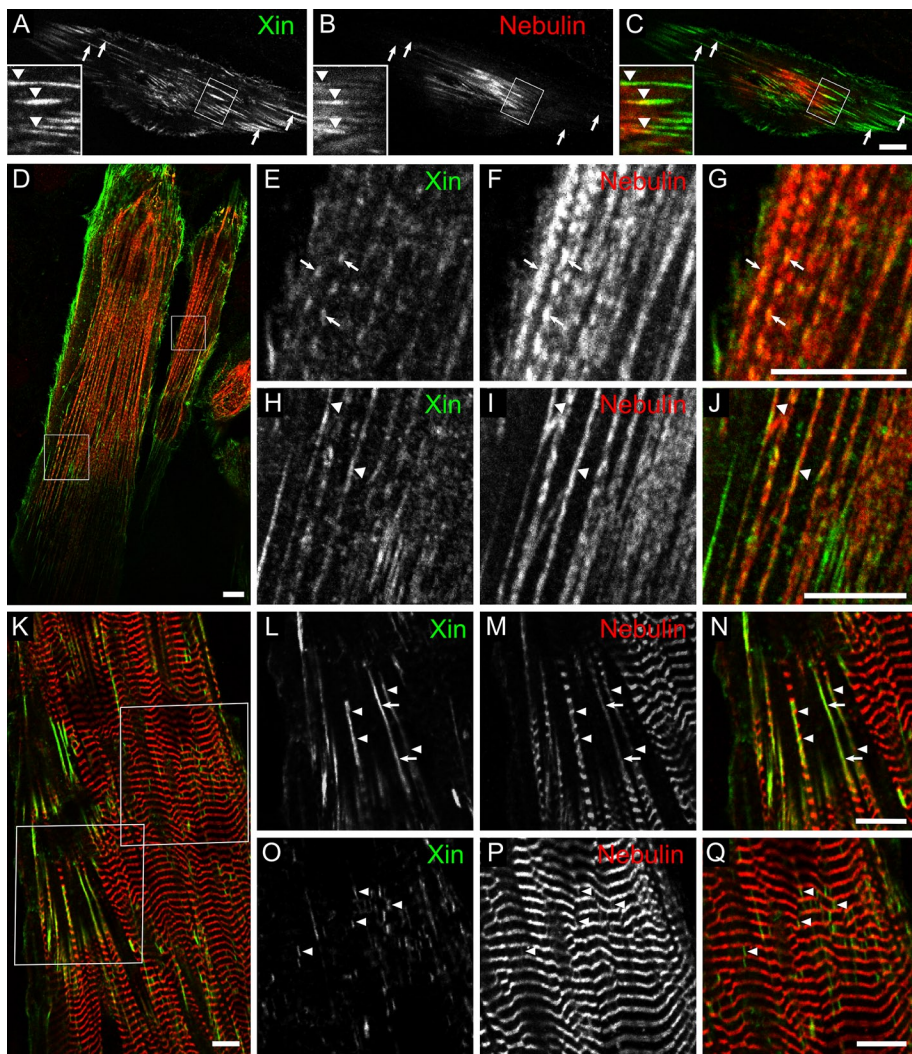
FIGURE 6: Immunolocalization of Xin and nebulin in differentiating mouse myocytes. Confocal laser scanning microscopy images of H-2K cells at different developmental stages stained with antibodies against Xin (A, E, H, L, O) and nebulin (B, F, I, M, P). In merged images (C, D, G, J, K, N, Q) Xin and nebulin are tinted green and red, respectively. Boxed areas in A–D and K are shown enlarged in insets (A–C) or in neighboring pictures (E–J, L–Q). In early-differentiating cells, Xin and nebulin partially colocalize along actin filament bundles (A–C, arrows; insets, arrowheads). More extensive colocalization is observed in nascent myofibrils (D; H–J, arrowheads). Xin weakly labels early myofibrils in a punctate pattern during developmental stages in which nebulin starts to be organized in Z-bodies (E–G, arrows). The colocalization seems to be lost on assembly of mature Z-discs that contain only nebulin (K–Q). In spontaneously contracting cells with cross-striated myofibrils (K–Q), Xin and nebulin colocalize in longitudinally oriented fibrillar structures that represent immature myofibrils or areas of remodeling (L–Q, arrowheads), whereas only nebulin is localized in Z-discs. Bar, 10 μm.

domains of nebulin and nebulette can be expected to exhibit overlapping binding partners. Indeed, we demonstrated that XIRP2 strongly interacts with both domains with affinities of 9.6 and 12.9 μM, respectively. These affinities are in a similar range to those of other predicted binding partners (Politou et al., 1998, 2002; Ma and Wang, 2002; Ma et al., 2006).

SH3 domains commonly represent interaction modules that generally recognize polyproline ligands comprising a minimal PXXP consensus motif (Kaneko et al., 2008). The interaction is mediated by a conserved central surface formed by the SH3 domain β-barrel, flanked by the RT and n-Src loops, which are more variable in sequence. Although polyproline ligands can bind to an SH3 domain in opposite orientations, directionality is frequently conferred by the interaction of a positively charged amino acid within its RT loop. Class I ligands bind the RT loop with a consensus motif +XXPXXP, in which "+" denotes a positively charged amino acid. In contrast, class II peptides, harboring the consensus sequence PXXPX+, bind the RT loop in an opposite orientation. The three-dimensional structure of the apo-nebulin SH3 domain suggests a preference for class II protein ligands (Politou et al., 1998, 2002). Considering the high sequence similarity of the nebulin and nebulette SH3 domains, it can be safely assumed that the ligand preferences are identical.

Because the binding regions in both human XIRPs contain several potential SH3 domain–binding motifs, we performed peptide array screening with nebulette's SH3 domain. We found a PPXXXPKP consensus motif to mediate the interaction, which is only in loose agreement with a class II peptide consensus, as the second proline is shifted by one position in comparison to the canonical class II PXXPX+ consensus. Our substitutional analysis revealed that presence of a positively charged residue in the C-terminal position is essential, and the preceding proline, although in a variable position of the canonical class II motif, is also strongly preferred. The second preference is more pronounced in the peptide scan data of the Xin motif than those of the XIRP2 motif. The structure of the nebulette–XIRP2 peptide confirms that the strongly preferred residues Pro-2250 and Lys-2251 provide most of the specific interactions with the SH3 domain (Figure 5). In contrast, Leu-2249, which is in a normally invariant proline position of the canonical PXXPX+, is not involved in specific interactions. The unusual positively charged residue cluster from the RT loop (residues 969–972) appears to be a strong determinant for the type of interactions observed in the nebulette–XIRP2 complex.

An important remaining question concerns where and when XIRPs interact with nebulin or nebulette in striated muscle cells. To get first insight into the biological significance of this interaction, we

motifs. Although the peptide exhibited modest affinity (6.2 μM) in in vitro binding assays, conclusive data about the precise binding mode necessary to evaluate the physiological relevance of these results are lacking (Ma and Wang, 2002).

Our study initially aimed at finding novel binding partners for a proline-rich region of Xin by performing yeast two-hybrid screens of a skeletal muscle cDNA library, yielding a large number of preys containing the nebulin SH3 domain. Because the two human XIRPs share a similar domain layout and considerable sequence homology, we tested the corresponding proline-rich region of XIRP2 and demonstrated that the interaction with this SH3 domain is common to both proteins. Similarly, the highly conserved (~75%) SH3
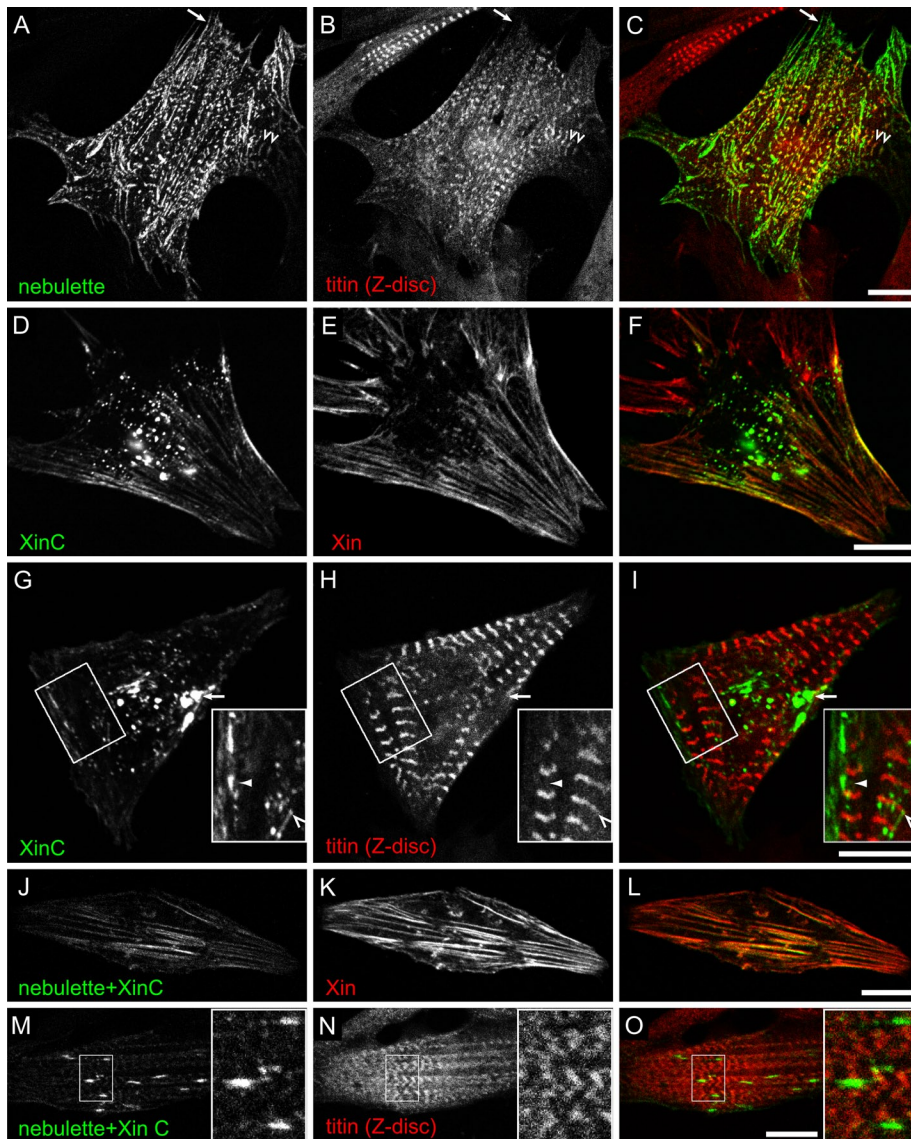
FIGURE 7: Transfection of embryonic mouse cardiomyocytes with XinC- and nebulette-encoding cDNAs. Venus-tagged nebulette targeted to nonstriated premyofibrils (arrow), whereas it colocalized with a Z-disc titin epitope (arrowheads) in regions exhibiting myofibrils (A–C). In contrast, XinC was prominently localized along premyofibrils, as indicated by staining of Xin (D–F), but not to Z-discs in further-differentiated cardiomyocytes. Note that the antibody used to stain Xin recognizes XinA and B but not XinC. In myofibrillar areas Xin specifically targeted to longitudinal strands between adjacent Z-discs identified by titin staining (G–I). Cotransfection of XinC and nebulette coupled to complementary nonfluorescent Venus fragments resulted in BiFC complex formation at premyofibrils of undifferentiated cells (J–L). In differentiated cardiomyocytes this complex became restricted to longitudinal strands between adjacent Z-discs (M–O). Bar, 10 μm.

confirmed targeting of nebulette to pre-myofibrils in a continuous way and to mature Z-discs (Moncman and Wang, 2002). XinC also localized in nascent myofibrils, whereas in differentiated stages it was restricted to longitudinal structures connecting adjacent Z-discs. Most important, the BiFC signal was revealed in only these locations, indicating a direct protein–protein interaction of nebulette (and, according to our immunolocalization experiments, also nebulin) with Xin in nascent myofibrils and longitudinal structures connecting mature Z-discs.

Because mainly the expression levels of both Xin isoforms containing the nebulin/nebulette binding site (XinA and XinC) are increased in pathologically altered human cardiac muscle (van der Ven *et al.*, 2006), a status accompanied by gross changes in cardiomyocyte architecture, these findings provide further evidence that Xin and nebulette interact during both myofibril formation and remodeling.

On treatment of zebrafish embryos with the acetylcholinesterase inhibitor galanthamine, the expression of Xirp1 is highly up-regulated. The protein is also immediately recruited to damaged areas and localizes to nascent myofibrils upon infliction of muscle damage with a laser (Otten *et al.*, 2012). Of interest, Xirp1 contains two sequences (PPILPKT and KPVIPPKP) compatible with the consensus sequence obtained for nebulin/nebulette-SH3 domain–binding proteins, and we were able to show that a Xirp1 fragment containing both regions indeed interacts with the SH3 domain of zebrafish nebulin (unpublished results).

The SH3 domain of nebulin is implicated in muscle hypertrophy via insulin-like growth factor 1 (IGF-1)–mediated recruitment of the actin polymerizer N-WASP to Z-discs (Takano *et al.*, 2010). It has been hypothesized that IGF-1 stimulation may lead to the release of the SH3 domain from binding to titin and CapZ, thus allowing interaction with other partners, such as N-WASP (Gautel and Ehler, 2010). Hypertrophic signals are expected to lead to the formation of new myofibrils, and thus Xin, which is found in premyofibrils, may be recruited by the exposed SH3 domain of nebulin. Once the myofibrils are fully developed, the SH3-mediated interaction may be inhibited, agreeing with the absence of Xin from mature sarcomeres.

Despite the partial differences in their distribution in adult muscle tissue, we provide here evidence that XIRPs are involved in muscle-remodeling processes. Both Xin and XIRP2 are prominent components of longitudinal strands that strongly resemble structures observed in human skeletal muscles recovering from myofibrillar damage inflicted by eccentric exercise (Yu and Thornell, 2002; Yu *et al.*, 2003, 2004; Carlsson *et al.*, 2008). Besides nebulin and

investigated the localization of Xin and the carboxy terminus of nebulin in differentiating cultured myotubes. Although both proteins did not colocalize in mature myofibrils, extensive colocalization was observed in premyofibrils and nascent myofibrils, indicating that this interaction is important for initial myofibrillar organization and not for their stabilization. The observed localization of nebulin in these structures together with sarcomeric α-actinin confirms the results of previous studies (Shimada *et al.*, 1996; Nwe *et al.*, 1999; Nwe and Shimada, 2000) and clearly identifies them as premyofibrils. This hypothesis was further investigated by analyzing the localization of Xin–nebulette complexes in myocytes using BiFC. This

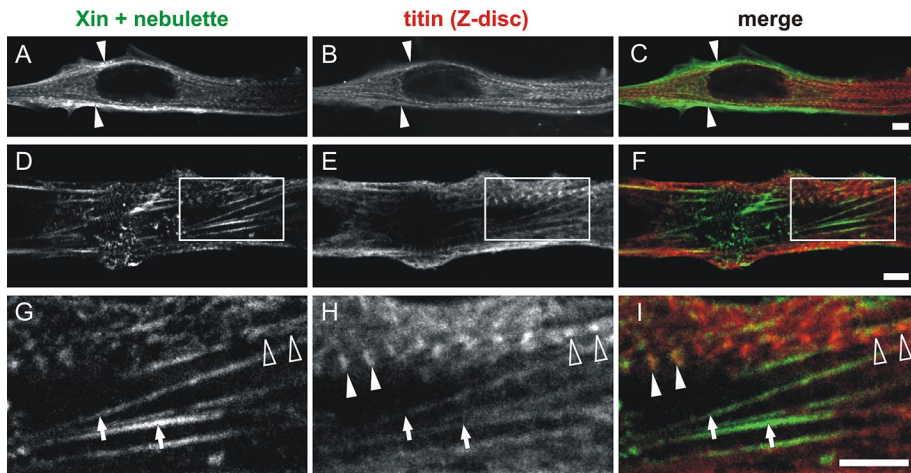| **Xin + nebulette**	**titin (Z-disc)**	**merge**

FIGURE 8: BiFC analysis of the interaction between XinB+PR4 and nebulette in C2C12 myocytes. BiFC complexes of Venus1-nebulette and XinB+PR4-Venus2 continuously decorate membrane-associated premyofibrils at early differentiation stages (A–C, arrows). In cells showing premyofibrils and nascent myofibrils with Z-bodies (D–I), the BiFC complex is continuously associated with these structures (G–I, arrows and open arrowheads, respectively). After the formation of striated myofibrils the complex is restricted to early Z-discs (G–I, closed arrowheads), whereas no signal is visible in mature Z-discs. (G–I) Magnification of the boxed areas in D–F. An antibody against a Z-disc epitope of titin was used to localize Z-discs. Bar, 10 μm.

nebulette, several other sarcomeric proteins, such as α-actinin and filamin C, interact with Xin and/or XIRP2 (Huang et al., 2006; van der Ven et al., 2006; Kley et al., 2013), which further supports the hypothesis that XIRPs are adapter proteins involved in targeting sarcomeric proteins to premyofibrils, Z-bodies, and, at a later developmental stage, also remodeling sarcomeres.

MATERIALS AND METHODS

Yeast two-hybrid assays

A human Xin cDNA fragment comprising amino acids 1120–1416 (PR3+4) was cloned into a modified pLex vector, and a human skeletal muscle cDNA library (Matchmaker cDNA library HL4047AH) was screened for interaction partners. Transformation into L40 yeast cells, culturing, and test for β-galactosidase activity were performed as described (van der Ven et al., 2000b). For submapping the interaction between Xin and nebulin and nebulette, one of the nebulin prey constructs and a nebulette construct covering the linker sequence and the SH3 domain (amino acids 851–1014) were tested for interaction with Xin fragments as described previously (van der Ven et al., 2006).

Bacterial expression constructs, purification, and coimmunoprecipitation of recombinant proteins

For biochemical verification of the Xin/XIRP2–nebulin/nebulette interaction, cDNA fragments of Xin, XIRP2, nebulin, and nebulette were cloned in pET23-EEF, pET23-T7 (Obermann et al., 1997), and pET23-myc. pET23-myc is derived from pET23-T7 by removing the T7 tag and replacing it by the myc-tag (EQKLISEEDL). This sequence is detected by the mouse monoclonal antibody (mAb) 9E10 (Evan et al., 1985; Schiweck et al., 1997). All constructs were transformed into E. coli strain BL21-CodonPlus(DE3)-RP (Stratagene, Santa Clara, CA), expressed, and purified as described before (Linnemann et al., 2010). Coimmunoprecipitation assays were carried out as described (Linnemann et al., 2010).

SDS–PAGE and Western blotting

SDS–PAGE was performed as described previously (Laemmli, 1970). Separated proteins were transferred to nitrocellulose membranes

(Roth, Karlsruhe, Germany) using a Transblot SD semidry blot apparatus (Bio-Rad, Munich, Germany). Transferred proteins were stained with Ponceau red before further processing. Primary antibodies used for immunostaining are described later. Horseradish peroxidase (HRP)–conjugated goat anti-mouse and goat anti-rat antibodies were purchased from Jackson ImmunoResearch/Dianova (Hamburg, Germany).

Peptide array screening

Peptide arrays were prepared on a cellulose-(3-amino-2-hydroxy-propyl)-ether membrane as previously described (Landgraf et al., 2004; Tonikian et al., 2009). Array design was generated using the in-house software LISA. To exclude false-positive spots in the incubation experiment, all cysteine residues were replaced by serine.

Probing synthetic peptide arrays for binding the GST-SH3 fusion proteins was performed as described previously (Landgraf et al., 2004; Tonikian et al., 2009). Briefly, a concentration of 10 μg/ml of each of the fusion proteins was used. Detection of GST-SH3 fusion protein binding was carried out using an anti-GST immunoglobulin G (IgG) antibody (Sigma G-1169, $c = 1$ μg/ml; Sigma-Aldrich, St. Louis, MO), followed by an anti-mouse IgG-HRP antibody (Sigma A 5906, $c = 1$ μg/ml) and a chemiluminescence substrate. Recording was done on a Lumi-Imager (Roche Diagnostics, Indianapolis, IN), and determination of SPOT signal intensities was executed with the software GeneSpotter (MicroDiscovery, Berlin, Germany).

Cardiomyocytes, cell culture, and transfection

Hearts of 16.5- to 18.5-d-old mouse embryos were dissected and briefly stored in cold phosphate-buffered saline (PBS). The hearts were minced and dissociated in enzyme solution containing 1 mg/ml collagenase B (Sigma-Aldrich) and 10 mM $CaCl_2$ for 30 min at 37°C. The collagenase was carefully aspirated, and sedimented cells were resuspended in cold PBS. Cell suspensions were passed through a 100-μm nylon mesh cell strainer (Life Technologies, Carlsbad, CA), and cells were collected in 50-ml tubes. After washing the cell strainer twice with cold PBS, cells were gently centrifuged, resuspended in 600 μl of cold PBS, and filled in a precooled electroporation cuvette (0.4-cm gap width; Bio-Rad). Plasmid DNA, 20 μg, was added, and cells were electroporated (240 V, $R = ∞$, $C = 500$ μF). Subsequently PBS was added to a final volume of 1.5 ml, and cells were distributed in three wells of a 24-well plate containing gelatin-coated glass coverslips and filled with culture medium (20% fetal calf serum [FCS], 2 mM ʟ-glutamine, 2 mM nonessential amino acids, 50 pM β-mercaptoethanol, 100 U/ml penicillin, and 100 μg/ml streptomycin in IMDM [Invitrogen, Carlsbad, CA]). Transfected cells were cultured for 2 d until they were fixed and stained.

Myoblasts derived from leg muscles of H-2Kb-tsA58 transgenic mice (Morgan et al., 1994) were cultured at 33°C in proliferation medium (20% FCS [PAA, Cölbe, Germany], 2% chicken embryo extract [Sera Laboratories International, Haywards Health, United Kingdom], 20 U/ml interferon-γ [Millipore, Billerica, CA], 100 U/ml penicillin, 100 μg/ml streptomycin, and DMEM with GlutaMAX [Life Technologies]) in culture dishes or on glass coverslips coated with BD Matrigel Basement Membrane Mix (BD Biosciences, Franklin,
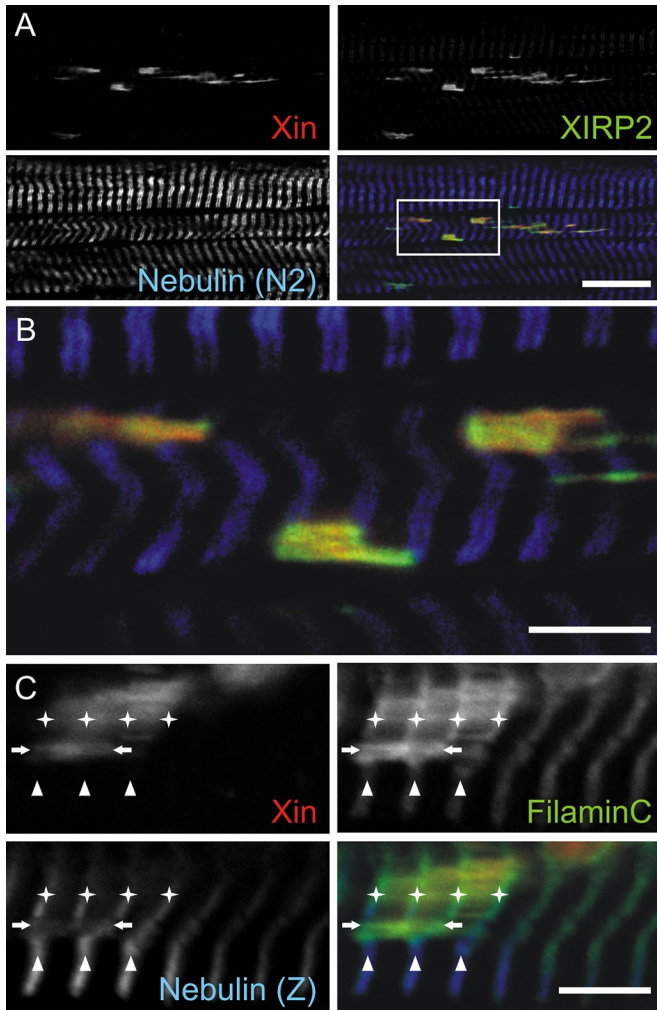
FIGURE 9: Immunolocalization of Xin, XIRP2, nebulin, and the Z-disc marker filamin C in mouse skeletal muscle sections. Sections were stained for Xin, XIRP2, and N2-line nebulin (A, B) or Xin, filamin C, and Z-disc nebulin, respectively (C). Xin is exclusively detected together with XIRP2 and filamin C along longitudinal strands between individual Z-discs. These areas of minor muscle damage show diffuse nebulin localization (A–C) that partially overlaps with Xin and filamin C (C, arrows). These regions often contain supernumerary sarcomeres, as indicated by the filamin C signal (compare asterisks and arrowheads in C). Bar, 20 µm (A), 5 µm (B, C).

NJ). Differentiation was induced by the replacement of the proliferation medium with differentiation medium (5% horse serum [Sigma-Aldrich], 100 U/ml penicillin, 100 µg/ml streptomycin in DMEM with GlutaMAX) and a switch to 37°C. Cells were allowed to differentiate for 1–9 d.

C2C12 cells were grown in proliferation medium (15% FCS, 100 U/ml penicillin, 100 µg/ml streptomycin, 2 mM nonessential amino acids, and 1 mM sodium pyruvate in DMEM with GlutaMAX). Cells were trypsinized and transfected using the Nucleofector technology using conditions suggested by the manufacturer (Lonza, Basel, Switzerland) for C2C12 cells. Cells were seeded on glass coverslips in proliferation medium and differentiated at 90% confluence by changing the medium to differentiation medium (2% horse serum, 100 U/ml penicillin, 100 µg/ml streptomycin, 2 mM nonessential amino acids, and 1 mM sodium pyruvate in DMEM with GlutaMAX). Cells were allowed to differentiate for up to 6 d.

Bimolecular fluorescence complementation

Bimolecular fluorescence complementation (Hu *et al.*, 2002) was used to visualize protein interactions in living cells. This assay is based on the association between two nonfluorescent fragments (Venus1 and Venus2: amino acids 1–154 and 155–238, respectively) of the yellow fluorescent protein Venus (Nagai *et al.*, 2002), each fused to one of two potential binding partners. We first constructed novel vectors enabling the expression of amino-terminal and carboxy-terminal Venus1 and Venus2 fusion proteins by replacing the DNA encoding enhanced green fluorescent protein (EGFP) in pEGFP-N3 or pEGFP-C1 (Clontech, Mountain View, CA) by Venus or one of the Venus fragments. For interaction assays, embryonic mouse cardiomyocytes or C2C12 mouse myoblasts were double transfected with Venus1 and Venus2 fusion proteins. All proteins were also transfected as full-length Venus fusion protein and cotransfected with the compatible nonfluorescent Venus fragments alone in order to evaluate unspecific BiFC complex formation. Cells were fixed and stained with applicable antibodies.

Antibodies and immunostaining

Described previously (Fürst *et al.*, 1988; van der Ven *et al.*, 2006; Claeys *et al.*, 2009) are the mouse mAbs XR1, recognizing XinA and B; XC1, recognizing XinA and C; XIRP2, raised against the carboxy terminus of human XIRP2; T12, decorating a titin epitope close to the Z-disc; and Nb2, decorating an epitope of nebulin close to the N2-line. The polyclonal rabbit antiserum (pAb) RaA653 detects sarcomeric α-actinin (van der Ven *et al.*, 2000a), and the pAb Nb m176-181 (a kind gift of C. Gregorio, University of Arizona, Tucson, AZ) labels a nebulin epitope close to the Z-disc (Conover *et al.*, 2009). The mAb against the T7 tag was purchased from Novagen (Heidelberg, Germany). Hybridoma cells producing mAb 9E10 recognizing the c-myc tag (Evan *et al.*, 1985; Schiweck *et al.*, 1997) were purchased from the American Type Culture Collection (Manassas, VA). The rat mAb YL1/2 (a kind gift of the late J. Wehland, Helmholtz Center, Braunschweig, Germany) was raised against the carboxy terminus of tyrosinated tubulin and recognizes the EEF tag (Wehland *et al.*, 1983). Goat anti-mouse and goat anti-rabbit secondary antibodies conjugated with Cy2, Cy3, and Cy5 were purchased from Jackson ImmunoResearch/Dianova.

Transfected cells were fixed with 4% paraformaldehyde for 10 min, followed by permeabilization with 0.05% Triton X-100 in PBS for 10 min or incubation with a 1:1 mixture of methanol and acetone for 5 min at –20°C. Frozen mouse or human skeletal muscle sections were fixed with methanol for 2 min at –20°C and subsequently with acetone for 20 s at –20°C. After washing with PBS, cells and sections were blocked with 10% normal goat serum and 1% bovine serum albumin (BSA) in PBS for 30 min at 37°C. The blocking reagent was removed, and primary antibodies diluted in 1% BSA in PBS were applied for 1–16 h. After washing three times with PBS, specimens were incubated with secondary antibodies diluted in 1% BSA in PBS, washed with PBS, and mounted in Mowiol containing 10% *N*-propyl gallate. Specimens were analyzed using a Zeiss LSM 710 confocal microscope or a Zeiss Cell Observer SD spinning disc microscope (Carl Zeiss, Jena, Germany).

Protein purification and crystallization

For crystallization and determination of binding affinities, the coding sequence of the nebulette SH3 domain (Uniprot O76041, residues 955–1014) was cloned between the *Nco*I and *Xho*I sites of the expression vector backbone pETM-11 to obtain an expression construct with an amino-terminal TEV protease-cleavable hexahistidine tag. Protein was expressed in *E. coli* BL21 star pRARE2

(Invitrogen/Novagen) under selection of kanamycin (50 µg/ml) and chloramphenicol (34 µg/ml) after induction with 0.5 mM isopropyl-β-D-thiogalactoside overnight at 20°C. Frozen, harvested cells were lysed by sonication in lysis buffer (20 mM Tris, pH 8.0, 250 mM NaCl, 1 µg/ml DNaseI), and the insoluble fraction was removed by centrifugation (30,000 × g for 1 h). The soluble fraction was applied to gravity-flow ion affinity chromatography columns and washed with lysis buffer containing 1 M NaCl, and bound protein was eluted in lysis buffer containing 250 mM imidazole. The hexahistidine tag was removed by incubation of the protein with TEV protease (1 mg of protease/50 mg of eluted protein) overnight at 4°C in lysis buffer. Cleaved protein was rebuffered into the crystallization buffer (20 mM Tris, pH 8.0, 150 mM NaCl) by size-exclusion chromatography on a Superdex 75 16/60 pg column (GE Healthcare, Piscataway, NJ).

The nebulette–XIRP2 complex was formed by mixing the recombinant SH3 domain (7 mg/ml) and a synthetic 13mer peptide derived from the XIRP2 recognition sequence (PPPTLPKPKLPKH, Uniprot A4UGR9 2245–2257) in a 1:2 M ratio. Crystallization screening was performed at the European Molecular Biology Laboratory [EMBL]-Hamburg high-throughput crystallization facility (Mueller-Dieckmann, 2006) in a sitting-drop vapor diffusion setup at constant 20°C. Crystals of the complex grew as clusters from drops containing a mixture of 200 nl of complex solution with 200 nl of precipitant solution (100 mM Tris, pH 8.0, 10 mM $ZnCl_2$, 20% polyethylene glycol [PEG] 6000) and reached their maximum size after ~3 wk.

Data collection, structure solution, and refinement

Diffraction data were collected at beamline X13 (EMBL-Hamburg/Deutsches Elektronen-Synchrotron). A small crystal fragment was separated from a cluster of crystals. It was soaked for 30 s in cryoprotectant solution (100 mM Tris, pH 8.0, 10 mM $ZnCl_2$, 30% PEG 6000) and directly flash-frozen to 100 K in the cryostream. High- and low-resolution diffraction data were collected in two separate steps from the same crystal, integrated separately with XDS, and scaled with Xscale (Kabsch, 2010). The structure was solved in the orthorhombic space group $P2_12_12_1$ by molecular replacement using the apo-nebulette SH3 domain as a model. Manual building of the protein coordinates was done in Coot, version 0.6.1 (Emsley and Cowtan, 2004). Maximum-likelihood refinement of atomic coordinates and anisotropic and isotropic B-factors was performed with Phenix, version 1.6.4-486 (Adams et al., 2010).

Determination of binding affinities

The synthetic peptide corresponding to the nebulin- and nebulette-binding region of XIRP2 (PPPTLPKPKLPKH) was dissolved at a concentration of 9 mM in water and then diluted to 750 µM in ITC buffer (Tris 12.5 mM, pH 8.0, NaCl 150 mM). Samples of purified nebulin and nebulette SH3 domains and synthetic XIRP2 peptides were dialyzed overnight against 4 l of ITC buffer at 4°C. All samples were preequilibrated at 25°C before starting the experiments. Titration experiments were carried out with a VP-ITC MicroCalorimeter from MicroCal (Northampton, MA). XIRP2 peptides were injected from the syringe into the sample cell containing nebulin or nebulette SH3 domains at 115–120 µM, resulting in a final 1:1.4 M ratio. All experiments were performed in triplicate at 25°C, using 10-µl injections every 240 ms. Data were corrected for injection and dilution effects by subtracting the basal heat remaining after saturation. Experimental data were analyzed using MicroCal Origin 7 software. Binding parameters (stoichiometry, affinities) were determined by fitting the data to a one-site binding mode using a nonlinear least-squares algorithm.

REFERENCES
Adams PD et al. (2010). PHENIX: a comprehensive Python-based system for macromolecular structure solution. Acta Crystallogr D Biol Crystallogr 66, 213–221.

Bang ML, Mudry RE, McElhinny AS, Trombitas K, Geach AJ, Yamasaki R, Sorimachi H, Granzier H, Gregorio CC, Labeit S (2001). Myopalladin, a novel 145-kilodalton sarcomeric protein with multiple roles in Z-disc and I-band protein assemblies. J Cell Biol 153, 413–427.

Carlsson L, Yu JG, Thornell LE (2008). New aspects of obscurin in human striated muscles. Histochem Cell Biol 130, 91–103.

Castillo A, Nowak R, Littlefield KP, Fowler VM, Littlefield RS (2009). A nebulin ruler does not dictate thin filament lengths. Biophys J 96, 1856–1865.

Claeys KG et al. (2009). Differential involvement of sarcomeric proteins in myofibrillar myopathies: a morphological and immunohistochemical study. Acta Neuropathol 117, 293–307.

Conover GM, Henderson SN, Gregorio CC (2009). A myopathy-linked desmin mutation perturbs striated muscle actin filament architecture. Mol Biol Cell 20, 834–845.

Emsley P, Cowtan K (2004). Coot: model-building tools for molecular graphics. Acta Crystallogr D Biol Crystallogr 60, 2126–2132.

Esham M, Bryan K, Milnes J, Holmes WB, Moncman CL (2007). Expression of nebulette during early cardiac development. Cell Motil Cytoskeleton 64, 258–273.

Evan GI, Lewis GK, Ramsay G, Bishop JM (1985). Isolation of monoclonal antibodies specific for human c-myc proto-oncogene product. Mol Cell Biol 5, 3610–3616.

Frank D, Frey N (2011). Cardiac Z-disc signaling network. J Biol Chem 286, 9897–9904.

Fürst DO, Osborn M, Nave R, Weber K (1988). The organization of titin filaments in the half-sarcomere revealed by monoclonal antibodies in immunoelectron microscopy: a map of ten nonrepetitive epitopes starting at the Z line extends close to the M line. J Cell Biol 106, 1563–1572.

Gautel M, Ehler E (2010). Cell biology. Gett'N-WASP stripes. Science 330, 1491–1492.

Gustafson-Wagner EA et al. (2007). Loss of mXinalpha, an intercalated disk protein, results in cardiac hypertrophy and cardiomyopathy with conduction defects. Am J Physiol Heart Circ Physiol 293, H2680–H2692.

Hawke TJ, Atkinson DJ, Kanatous SB, van der Ven PFM, Goetsch SC, Garry DJ (2007). Xin, an actin binding protein, is expressed within muscle satellite cells and newly regenerated skeletal muscle fibers. Am J Physiol Cell Physiol 293, C1636–C1644.

Hu CD, Chinenov Y, Kerppola TK (2002). Visualization of interactions among bZIP and Rel family proteins in living cells using bimolecular fluorescence complementation. Mol Cell 9, 789–798.

Huang HT, Brand OM, Mathew M, Ignatiou C, Ewen EP, McCalmon SA, Naya FJ (2006). Myomaxin is a novel transcriptional target for MEF2A that encodes a Xin related alpha-actinin interacting protein. J Biol Chem 281, 39370–39379.

Joo YM et al. (2004). Identification of chicken nebulin isoforms of the 31-residue motifs and non-muscle nebulin. Biochem Biophys Res Commun 325, 1286–1291.

Kabsch W (2010). XDS. Acta Crystallogr D Biol Crystallogr 66, 125–132.

Kaneko T, Li L, Li SS (2008). The SH3 domain—a family of versatile peptide- and protein-recognition module. Front Biosci 13, 4938–4952.

Kazmierski ST, Antin PB, Witt CC, Huebner N, McElhinny AS, Labeit S, Gregorio CC (2003). The complete mouse nebulin gene sequence and the identification of cardiac nebulin. J Mol Biol 328, 835–846.

Kley RA et al. (2013). A combined laser microdissection and mass spectrometry approach reveals new disease relevant proteins accumulating in aggregates of filaminopathy patients. Mol Cell Proteomics 12, 215–227.

Labeit S, Gibson T, Lakey A, Leonard K, Zeviani M, Knight P, Wardale J, Trinick J (1991). Evidence that nebulin is a protein-ruler in muscle thin filaments. FEBS Lett 282, 313–316.

Labeit S, Kolmerer B (1995). The complete primary structure of human nebulin and its correlation to muscle structure. J Mol Biol 248, 308–315.

Laemmli UK (1970). Cleavage of structural proteins during the assembly of the head of bacteriophage T4. Nature 227, 680–685.

Landgraf C, Panni S, Montecchi-Palazzi L, Castagnoli L, Schneider-Mergener J, Volkmer-Engert R, Cesareni G (2004). Protein interaction networks by proteome peptide scanning. PLoS Biol 2, E14.

Li B, Zhuang L, Trueb B (2004). Zyxin interacts with the SH3 domains of the cytoskeletal proteins LIM-nebulette and Lasp-1. J Biol Chem 279, 20401–20410.

Linnemann A, van der Ven PFM, Vakeel P, Albinus B, Simonis D, Bendas G, Schenk JA, Micheel B, Kley RA, Fürst DO (2010). The sarcomeric Z-disc component myopodin is a multiadapter protein that interacts with filamin and alpha-actinin. Eur J Cell Biol 89, 681–692.

Luther PK (2009). The vertebrate muscle Z-disc: sarcomere anchor for structure and signalling. J Muscle Res Cell Motil 30, 171–185.

Ma K, Forbes JG, Gutierrez-Cruz G, Wang K (2006). Titin as a giant scaffold for integrating stress and Src homology domain 3-mediated signaling pathways: the clustering of novel overlap ligand motifs in the elastic PEVK segment. J Biol Chem 281, 27539–27556.

Ma K, Wang K (2002). Interaction of nebulin SH3 domain with titin PEVK and myopalladin: implications for the signaling and assembly role of titin and nebulin. FEBS Lett 532, 273–278.

McCalmon SA et al. (2010). Modulation of angiotensin II-mediated cardiac remodeling by the MEF2A target gene Xirp2. Circ Res 106, 952–960.

McElhinny AS, Kolmerer B, Fowler VM, Labeit S, Gregorio CC (2001). The N-terminal end of nebulin interacts with tropomodulin at the pointed ends of the thin filaments. J Biol Chem 276, 583–592.

McElhinny AS, Schwach C, Valichnac M, Mount-Patrick S, Gregorio CC (2005). Nebulin regulates the assembly and lengths of the thin filaments in striated muscle. J Cell Biol 170, 947–957.

Millevoi S, Trombitas K, Kolmerer B, Kostin S, Schaper J, Pelin K, Granzier H, Labeit S (1998). Characterization of nebulette and nebulin and emerging concepts of their roles for vertebrate Z-discs. J Mol Biol 282, 111–123.

Moncman CL, Wang K (1999). Functional dissection of nebulette demonstrates actin binding of nebulin-like repeats and Z-line targeting of SH3 and linker domains. Cell Motil Cytoskeleton 44, 1–22.

Moncman CL, Wang K (2002). Targeted disruption of nebulette protein expression alters cardiac myofibril assembly and function. Exp Cell Res 273, 204–218.

Morgan JE, Beauchamp JR, Pagel CN, Peckham M, Ataliotis P, Jat PS, Noble MD, Farmer K, Partridge TA (1994). Myogenic cell lines derived from transgenic mice carrying a thermolabile T antigen: a model system for the derivation of tissue-specific and mutation-specific cell lines. Dev Biol 162, 486–498.

Mueller-Dieckmann J (2006). The open-access high-throughput crystallization facility at EMBL Hamburg. Acta Crystallogr D Biol Crystallogr 62, 1446–1452.

Nagai T, Ibata K, Park ES, Kubota M, Mikoshiba K, Miyawaki A (2002). A variant of yellow fluorescent protein with fast and efficient maturation for cell-biological applications. Nat Biotechnol 20, 87–90.

Nave R, Fürst DO, Weber K (1990). Interaction of alpha-actinin and nebulin in vitro. Support for the existence of a fourth filament system in skeletal muscle. FEBS Lett 269, 163–166.

Nwe TM, Maruyama K, Shimada Y (1999). Relation of nebulin and connectin (titin) to dynamics of actin in nascent myofibrils of cultured skeletal muscle cells. Exp Cell Res 252, 33–40.

Nwe TM, Shimada Y (2000). Inhibition of nebulin and connectin (titin) for assembly of actin filaments during myofibrillogenesis. Tissue Cell 32, 223–227.

Obermann WMJ, Gautel M, Weber K, Fürst DO (1997). Molecular structure of the sarcomeric M band: mapping of titin and myosin binding domains in myomesin and the identification of a potential regulatory phosphorylation site in myomesin. EMBO J 16, 211–220.

Otten C et al. (2012). XIRP proteins mark injured skeletal muscle in zebrafish. PLoS ONE 7, e31041.

Otten J et al. (2010). Complete loss of murine Xin results in a mild cardiac phenotype with altered distribution of intercalated discs. Cardiovasc Res 85, 739–750.

Pacholsky D, Vakeel P, Himmel M, Löwe T, Stradal T, Rottner K, Fürst DO, van der Ven PFM (2004). Xin repeats define a novel actin-binding motif. J Cell Sci 117, 5257–5268.

Panaviene Z, Moncman CL (2007). Linker region of nebulin family members plays an important role in targeting these molecules to cellular structures. Cell Tissue Res 327, 353–369.

Pappas CT, Bliss KT, Zieseniss A, Gregorio CC (2011). The nebulin family: an actin support group. Trends Cell Biol 21, 29–37.

Pappas CT, Krieg PA, Gregorio CC (2010). Nebulin regulates actin filament lengths by a stabilization mechanism. J Cell Biol 189, 859–870.

Politou AS, Millevoi S, Gautel M, Kolmerer B, Pastore A (1998). SH3 in muscles: solution structure of the SH3 domain from nebulin. J Mol Biol 276, 189–202.

Politou AS, Spadaccini R, Joseph C, Brannetti B, Guerrini R, Helmer-Citterich M, Salvadori S, Temussi PA, Pastore A (2002). The SH3 domain of nebulin binds selectively to type II peptides: theoretical prediction and experimental validation. J Mol Biol 316, 305–315.

Purevjav E et al. (2010). Nebulette mutations are associated with dilated cardiomyopathy and endocardial fibroelastosis. J Am Coll Cardiol 56, 1493–1502.

Rhee D, Sanger JM, Sanger JW (1994). The premyofibril: evidence for its role in myofibrillogenesis. Cell Motil Cytoskeleton 28, 1–24.

Sanger JW, Chowrashi P, Shaner NC, Spalthoff S, Wang J, Freeman NL, Sanger JM (2002). Myofibrillogenesis in skeletal muscle cells. Clin Orthop Relat Res S153-S162.

Sanger JW, Wang J, Fan Y, White J, Sanger JM (2010). Assembly and dynamics of myofibrils. J Biomed Biotechnol 2010, 858606.

Schiweck W, Buxbaum B, Schatzlein C, Neiss HG, Skerra A (1997). Sequence analysis and bacterial production of the anti-c-myc antibody 9E10: the V(H) domain has an extended CDR-H3 and exhibits unusual solubility. FEBS Lett 414, 33–38.

Shimada Y, Komiyama M, Begum S, Maruyama K (1996). Development of connectin/titin and nebulin in striated muscles of chicken. Adv Biophys 33, 223–233.

Takano K, Watanabe-Takano H, Suetsugu S, Kurita S, Tsujita K, Kimura S, Karatsu T, Takenawa T, Endo T (2010). Nebulin and N-WASP cooperate to cause IGF-1-induced sarcomeric actin filament formation. Science 330, 1536–1540.

Tonikian R et al. (2009). Bayesian modeling of the yeast SH3 domain interactome predicts spatiotemporal dynamics of endocytosis proteins. PLoS Biol 7, e1000218.

van der Ven PFM, Ehler E, Vakeel P, Eulitz S, Schenk JA, Milting H, Micheel B, Fürst DO (2006). Unusual splicing events result in distinct Xin isoforms that associate differentially with filamin C and Mena/VASP. Exp Cell Res 312, 2154–2167.

van der Ven PFM, Obermann WMJ, Lemke B, Gautel M, Weber K, Fürst DO (2000a). Characterization of muscle filamin isoforms suggests a possible role of γ-filamin/ABP-L in sarcomeric Z-disc formation. Cell Motil Cytoskeleton 45, 149–162.

van der Ven PFM et al. (2000b). Indications for a novel muscular dystrophy pathway. γ-Filamin, the muscle-specific filamin isoform, interacts with myotilin. J Cell Biol 151, 235–248.

Wang DZ, Reiter RS, Lin JL, Wang Q, Williams HS, Krob SL, Schultheiss TM, Evans S, Lin JJ (1999). Requirement of a novel gene, Xin, in cardiac morphogenesis. Development 126, 1281–1294.

Wang Q et al. (2010). Essential roles of an intercalated disc protein, mXinbeta, in postnatal heart growth and survival. Circ Res 106, 1468–1478.

Wehland J, Willingham MC, Sandoval IV (1983). A rat monoclonal antibody reacting specifically with the tyrosylated form of alpha-tubulin. I. Biochemical characterization, effects on microtubule polymerization in vitro, and microtubule polymerization and organization in vivo. J Cell Biol 97, 1467–1475.

Witt CC, Burkart C, Labeit D, McNabb M, Wu Y, Granzier H, Labeit S (2006). Nebulin regulates thin filament length, contractility, and Z-disk structure in vivo. EMBO J 25, 3843–3855.

Wright J, Huang QQ, Wang K (1993). Nebulin is a full-length template of actin filaments in the skeletal muscle sarcomere: an immunoelectron microscopic study of its orientation and span with site-specific monoclonal antibodies. J Muscle Res Cell Motil 14, 476–483.

Yu JG, Carlsson L, Thornell LE (2004). Evidence for myofibril remodeling as opposed to myofibril damage in human muscles with DOMS: an ultrastructural and immunoelectron microscopic study. Histochem Cell Biol 121, 219–227.

Yu JG, Fürst DO, Thornell LE (2003). The mode of myofibril remodelling in human skeletal muscle affected by DOMS induced by eccentric contractions. Histochem Cell Biol 119, 383–393.

Yu JG, Thornell LE (2002). Desmin and actin alterations in human muscles affected by delayed onset muscle soreness: a high resolution immunocytochemical study. Histochem Cell Biol 118, 171–179.

Zieseniss A, Terasaki AG, Gregorio CC (2008). Lasp-2 expression, localization, and ligand interactions: a new Z-disc scaffolding protein. Cell Motil Cytoskeleton 65, 59–72.